Supporting Information

A phthalocyanine-based polycrystalline interlayer simultaneously realizing charge collection and ion defect passivation for perovskite solar cells

Tatsuya Ohsawa,[a*] Naoyuki Shibayama,[b*] Nobuhiro Nakamura,[a] Shigeto Tamura,[a] Ai Hayakawa,[a] Yohei Murayama,[a] Kohei Makisumi,[a] Michitaka Kitahara,[a] Mizuki Takayama,[a] Takashi Matsui,[a] Atsushi Okuda,[a] Yuiga Nakamura,[c] Masashi Ikegami,[b] and Tsutomu Miyasaka[b]

a. Specialty Chemicals Development Center, Peripheral Products Operations, Canon Inc. 30-2, Shimomaruko 3-chome, Ohta-ku, Tokyo, Japan
E-mail: ohsawa.tatsuya@mail.canon

b. Graduate School of Engineering, Toin University of Yokohama, 1614 Kuroganecho, Aoba, Yokohama, Kanagawa, Japan
E-mail: shibayama@toin.ac.jp

c. Japan Synchrotron Radiation Research Institute/SPring-8, 1-1-1 Kouto, Sayo, Hyogo, Japan

Experiment Section

***Materials**:* Lead Iodide (PbI_2), lead bromide ($PbBr_2$), formamidine hydroiodide (FAI), formamidine bromide (FABr), methylamine hydroiodide (MAI) and methylamine bromide (MABr) were purchased from Tokyo Chemical Industry. Dimethyl sulfoxide (DMSO, 99.9%), and *N, N*-Dimethylformamide (DMF, 99.8%) were purchased from FUJIFILM Wako Pure Chemical Corporation. Tin (IV) Oxide (SnO_2), 15% in H_2O colloidal dispersion was purchased from Alfa Aesar. BM-2 was purchased from Sekisui Chemical Co. LTD. Two synthesized compounds were used: Gallium phthalocyanine hydroxide (OHGaPc) and a Calix[4]arene derivatives (CA), with synthesis details reported in Japanese Patent Applications 2018-189957 and 2003-207913, respectively. 2,2',7,7'-Tetrakis-(*N,N*-di-4-methoxyphenylamino)-9,9'-spirobifluorene (spiro-OMeTAD, >99.9%) was purchased from Nippon Fine Chemical Co., LTD. All solvents and reagents were of the highest quality available and were used as received.

***Device Fabrication**:* The ITO-coated glass (≤10 Ω/sq, Geomatec Co.) was cleaned by sonicating the substrates 15 min in (1) a solution of 2% Cica Clean LX-II, (2) deionized water, (3) acetone, and (4) isopropyl alcohol (IPA). Dried ITO substrates were treated in UV-Ozone cleaner (ASM401oz, Asumigiken, LTD.) for 10 min. SnO_2 colloid dispersion was diluted by H_2O with the volume ratio of 1/7 and was spin-coated onto ITO/glass substrate at 5000 rpm for 30 s, and then baked on a hot plate at 150 ^oC for 30 min. The coatings were then dried in a drying room at a humidity such that the dew point temperature was −20°C. To form the perovskite layer, a perovskite precursor solution was prepared with a lead excess $Cs_{0.1}(FA_{0.87}MA_{0.13})_{0.9}Pb(I_{0.9}Br_{0.1})_3$ by mixing lead iodide (1.2 M), lead bromide (0.15 M), formamidinium iodide (1.0 M), methylammonium bromide (0.15 M), and cesium iodide (0.13 M) in DMF : DMSO = 4 : 1 (volume ratio). The perovskite solution was spun on the substrate with a two-step spin-coating program set at 2700 and 5000 rpm for 10 and 20 s, respectively. During spin-coating, 150 μL of chlorobenzene was dripped on the substrate 5 s before the termination time of the spin-coating. Then, the substrate was annealed at 130 °C for 15min to crystallize the perovskite layer. After that, a solution of OHGaPc diluted in IPA was spun on the substrate at 1,000 rpm for 30 s followed by drying in air at 60°C for 10 minutes. The OHGaPc solution was obtained by dispersing 0.1 g of OHGaPc, 0.01 g of CA, and 0.01 g of BM-2 in 10.8 g (thickness of OHGaPc film = 130 nm), and 7.88 g (250 nm), 5.89 g (350 nm), 4.69 g (400 nm), 3.89 g (600 nm) of IPA, respectively. To deposit the hole-

transport material (HTM), 80 mg of spiro-OMeTAD solution was diluted in 1023 µL of chlorobenzene, followed by adding 32 µL of 4-*tert*-butylpyridine, 19 µL of bis(trifluoromethane)sulfonimide lithium salt solution (517 mg mL^{-1}) in acetonitrile, and 14 µL of cobalt-complex solution (376 mg mL^{-1}) in acetonitrile. The prepared spiro-OMeTAD solution was spun on the substrate at 2000 rpm for 30 s. Last, a 70 nm Au layer was deposited on the spiro-OMeTAD layer as a counter electrode. During Au evaporation, a metal pattern plate was used for controlling the aperture area (0.09 cm^2).

Characterizations*:* Nuclear Magnetic Resonance (NMR) measurements were performed using a Bruker CryoProbe NMR system operating at 600 MHz, provided by Bruker Corporation. The ^{1}H-NMR experiments involved a rotation speed of 20 Hz with accumulation of 256 scans to enhance signal clarity. The X-ray photoelectron spectroscopy (XPS) measurements were carried out on a PHI Quantes (Ulvac-PHI Inc.) with a monochromator and a source of Al-Kα 1486.6 eV. The spectrum was referenced using the C–C bound component of adventitious carbon. An ultraviolet photoelectron spectrometer (UPS) equipped with a He–I source (hv = 21.22 eV) (AXIS Nova, Kratos Analytical Ltd, UK) was used to determine the valence band energy and Fermi-level. The Fermi-level of the samples was referenced to that of Au which was in electrical contact with a sample in UPS measurements. Two-dimensional grazing incidence wide-angle X-ray scattering (2D-GIWAXS) patterns represented in reciprocal lattice space were conducted at SPring-8 on beamline BL19B2. The sample was irradiated with an X-ray energy of 12.39 keV (λ = 1 Å) at a fixed incident angle on the order of 0.12° through a Huber diffractometer. The 2D-GIWAXS patterns were recorded with a two-dimensional image detector (Pilatus 300 K). Photoluminescence studies, encompassing both steady-state and time-resolved photoluminescence (SSPL and TRPL), utilized a Quantaurus-Tau C11367 spectrometer from Hamamatsu Photonics. The excitation source for these measurements was a PLP-10-065TAU, controlled by a C10196 controller, with an excitation wavelength of 655 nm. SSPL measurements were conducted at a 10 MHz repetition rate, while TRPL experiments utilized a 50 kHz frequency. The PEC solar simulator (LED light, Peccell Technologies) with the light intensity of 100 mW cm^{-2} was used as light source and Keithley 2400 source meter was used for current density-voltage (*J-V*) measurements of solar cells. The power of the light exposure from the solar simulator was calibrated using standard Si cell (BS-520, Bunkoukeiki Co., Ltd.) whose mismatch was corrected by spectral sensitivity characteristics. The active area was determined by the photomasks (0.09 cm^2 for 0.09 cm^2-aperture area) placed in front of

the glass side of the solar cell. Measurements of some perovskite devices and incident photon-to-current conversion efficiency measurements (IPCE) were performed by Kanagawa Institute of Industrial Science and Technology (KISTEC), a third-party measurement organization (Figure S10). For the durability testing of devices without encapsulation under light irradiation, an experimental setup comprising a white light LED source, PS-LED2+LED-BOX-6570, was used, supplied by Nippon PI Co., Ltd. Temperature control during the experiments was achieved using a BN-VT300K jet cooler from Nippon Precision Instruments Co., Ltd. Data logging was performed using an LR8431 datalogger from HIOKI E.E. Corporation, enabling simultaneous voltage measurements and logging. The devices were fabricated on 25 x 25 mm square glass substrates with each layer deposited to form 3x3 mm square cells. The light irradiation was set to approximately 110,000 lux to match the photocurrent generation equivalent to 1 sun intensity in a solar simulator. Each channel was connected to a circuit as shown in diagram as shown in Figure S12, with a load resistance (VR) of 100 Ω. The voltage across each channel's circuit was measured and logged using the datalogger capable of DC voltage measurements. By applying Ohm's law (V = RI), the output current was calculated, allowing for the assessment of the devices' durability performance over time under light exposure, with the device temperature controlled to remain at 32°C within an atmospheric evaluation box. Scanning Electron Microscopy (SEM) analysis was carried out using a Gemini SEM 560 from Carl Zeiss Co., Ltd., at an acceleration voltage of 1.0 kV. Time-of-Flight Secondary Ion Mass Spectrometry (TOF-SIMS) experiments were performed on a PHI nanoTOF II system, supplied by ULVAC-PHI, INC. Sputtering conditions involved Ar cluster ions ($Ar2000^+$) at an acceleration voltage of 10kV, and sputter interval of 2 seconds. Analysis conditions included the use of Bi^+ primary ions at 30kV in bunched mode, detection of negative secondary ions, a scan area of 100×100μm², and electron beam neutralization at 15V. The TOF-SIMS analysis focused on tracking the intensity of ions such as I^-, Br^-, spiro-$OMeTAD^-$, and $OHGaPc^-$ across the device interior. The measurements were taken after peeling off the gold electrode and performing depth profiling with Ar-cluster sputtering.

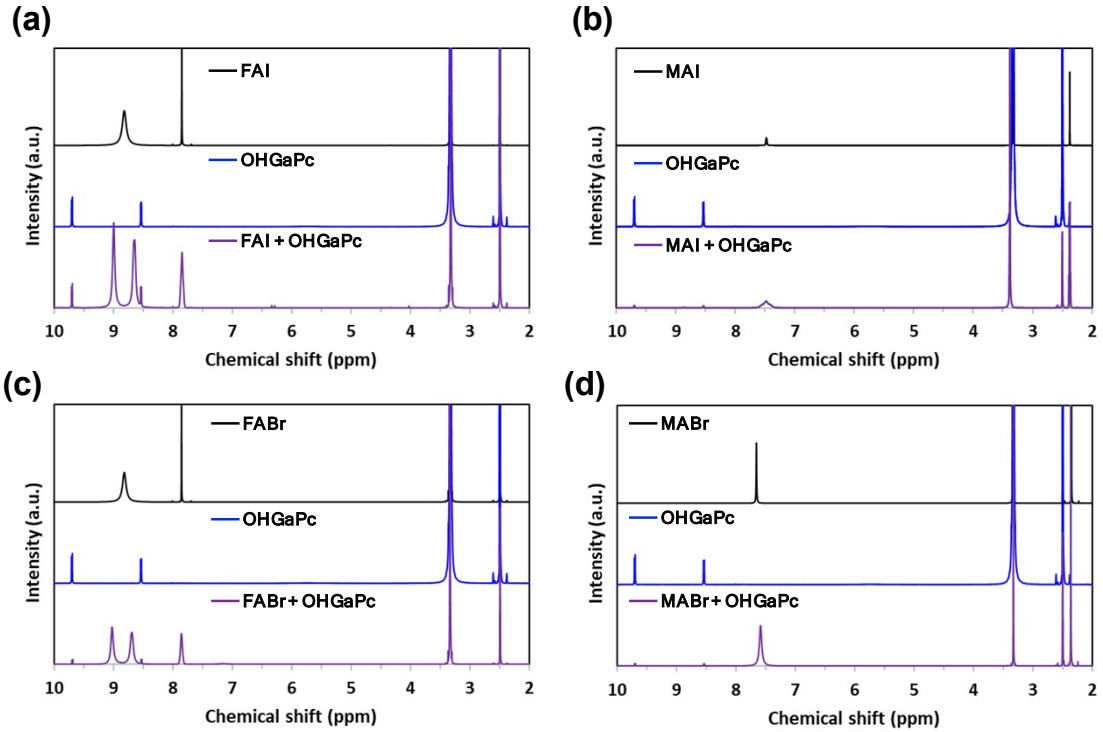

Fig. S1 Wide-range ^{1}H-NMR spectra of OHGaPc with perovskite precursor materials (a) FAI, (b) MAI, (c) FABr, and (d) MABr with and without OHGaPc.

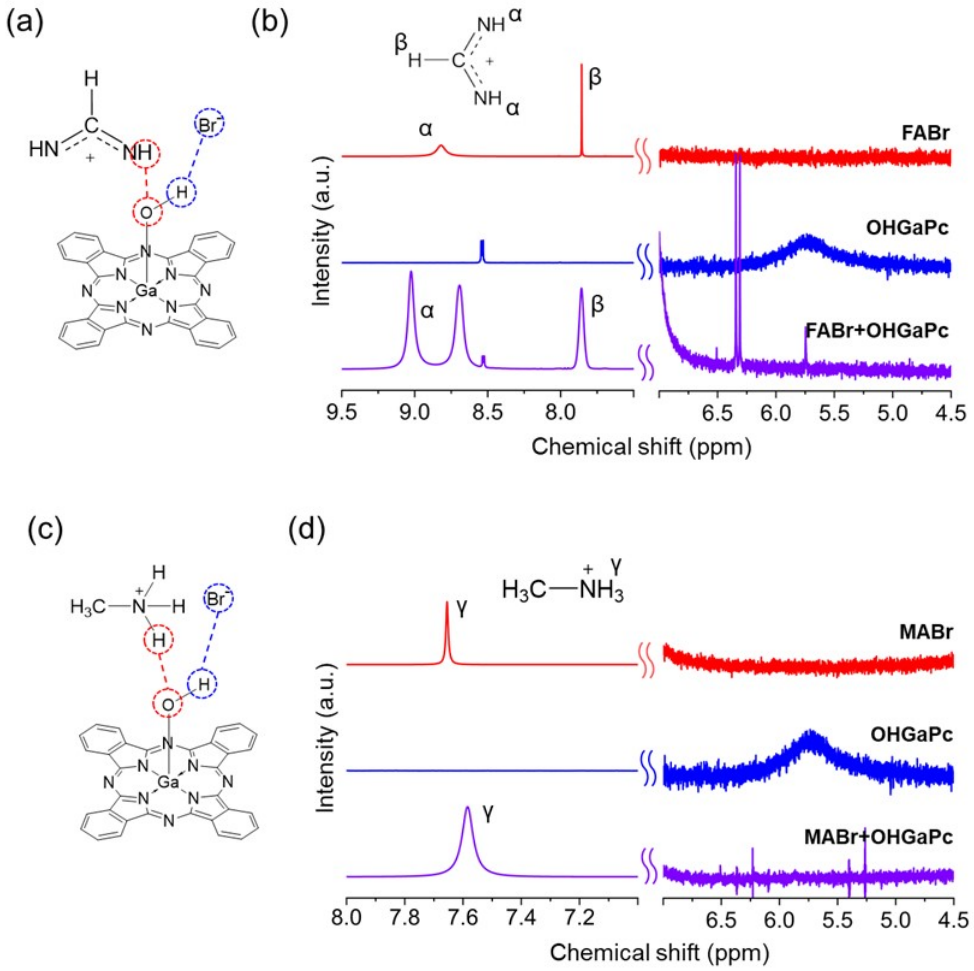

Fig. S2 Schematics and liquid-state partial ^{1}H-NMR spectra of OHGaPc with perovskite precursor materials FABr and MABr. (a) and (b) pertain to FABr with OHGaPc; (c) and (d) to MABr with OHGaPc.

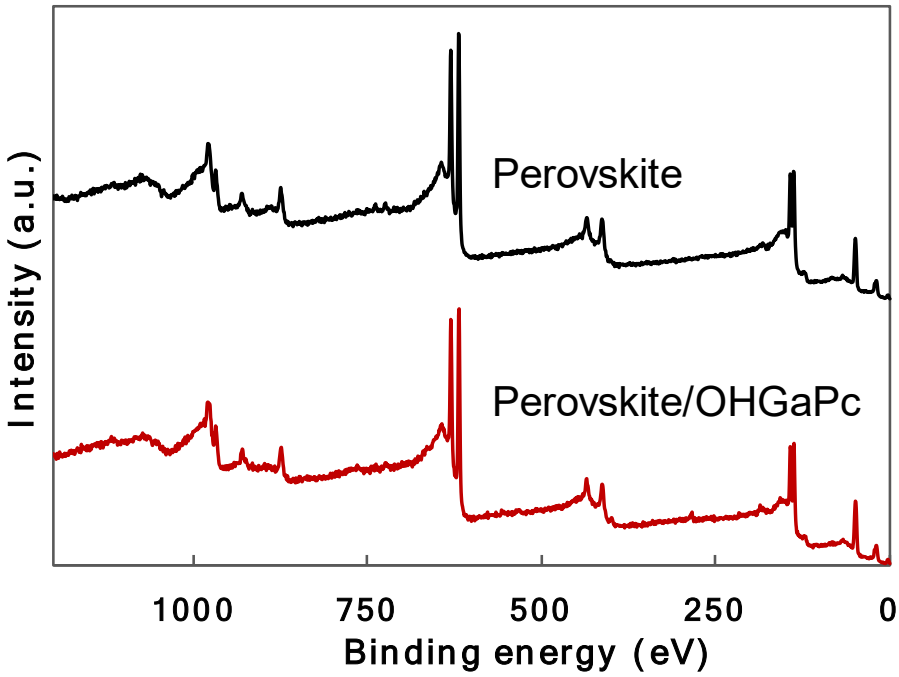

Fig. S3 XPS spectra of the perovskite thin films with and without OHGaPc.

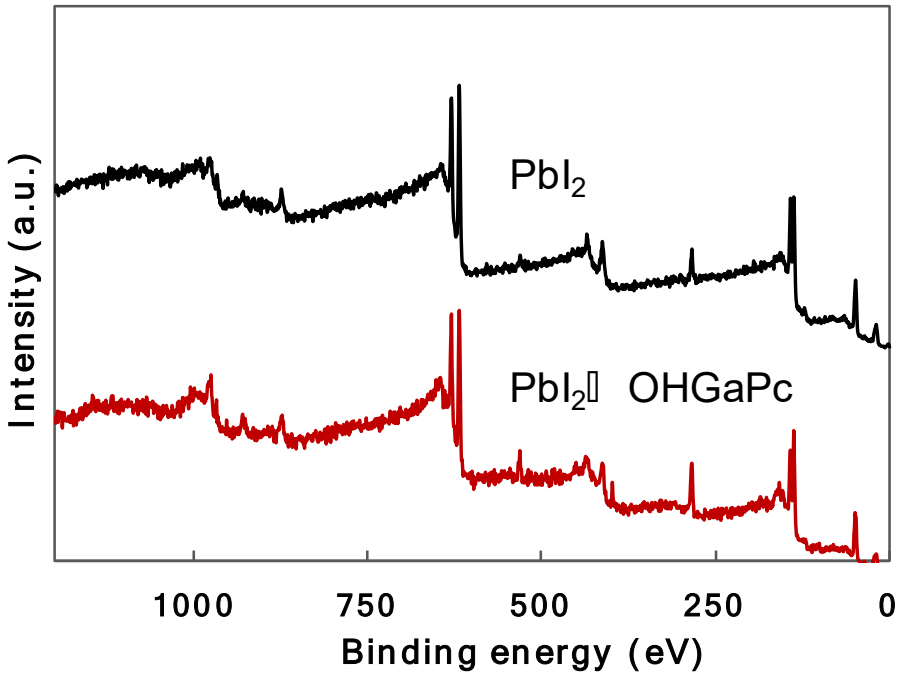

Fig. S4 XPS spectra of the perovskite thin films with and without OHGaPc.

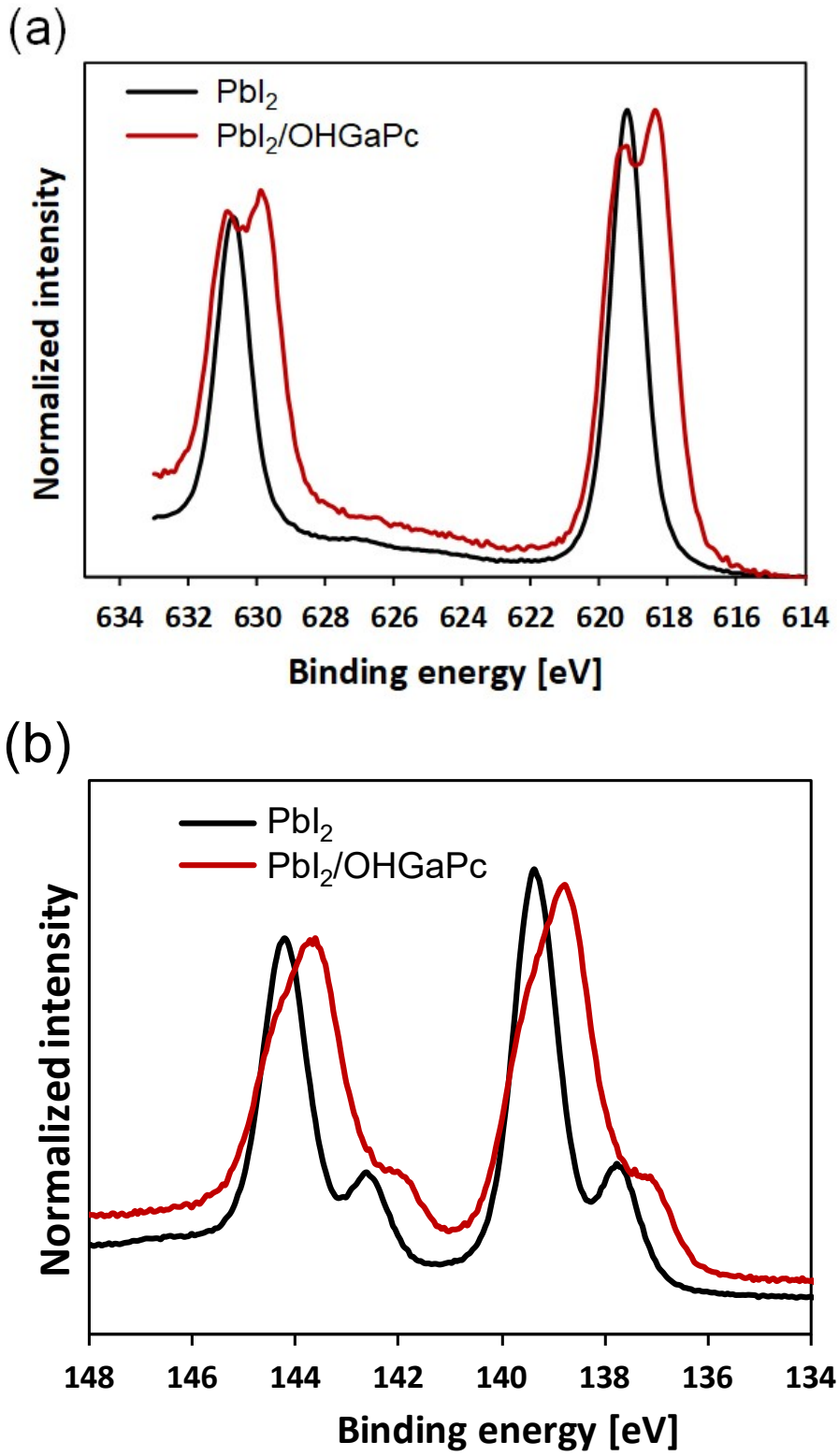

Fig. S5 XPS spectra of PbI_2 with and without OHGaPc (a) for Pb for Pb $4f_{7/2}$ and Pb $4f_{5/2}$ peaks, (b) for I $3d_{5/2}$ and I $3d_{3/2}$ peaks.

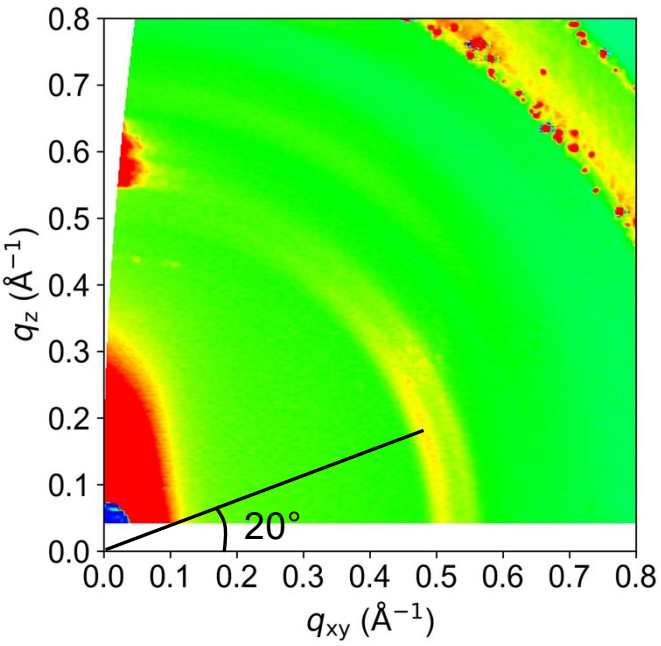

Fig. S6 GIWAXS pattern of the OHGaPc layer on the perovskite thin film.

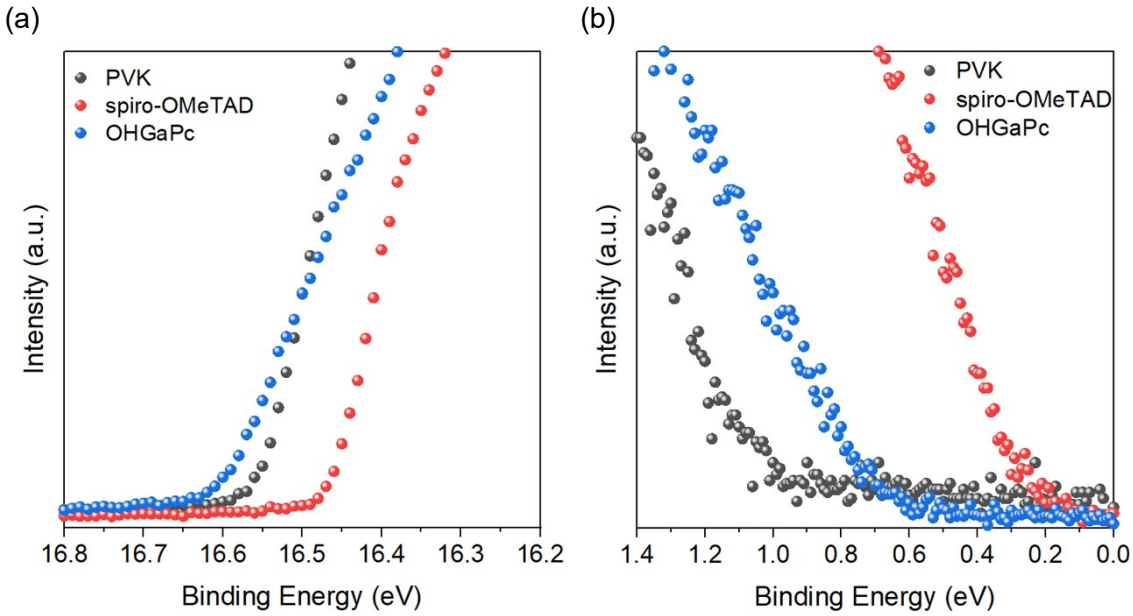

Fig. S7 UPS spectra of the perovskite, spiro-OMeTAD, and OHGaPc films around (a) the edge of the work function and (b) the valence band edge. The work function values were calculated by subtracting 21.22 eV from the spectrum edge of Fig. S7a.

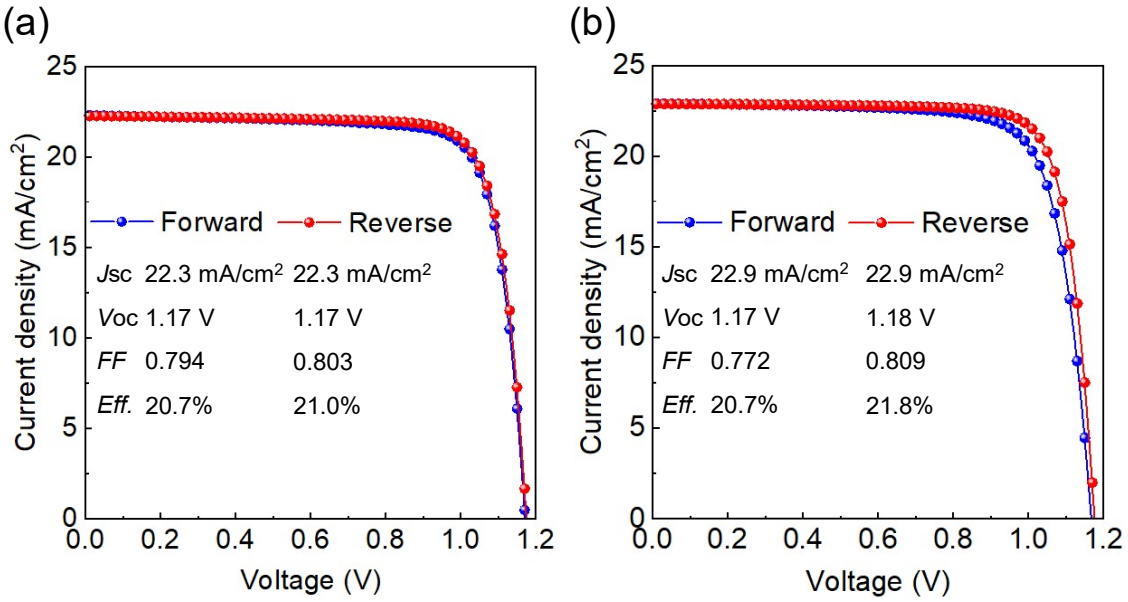

Fig. S8 *J-V* curves of perovskite solar cells (a) with and (b) without OHGaPc.

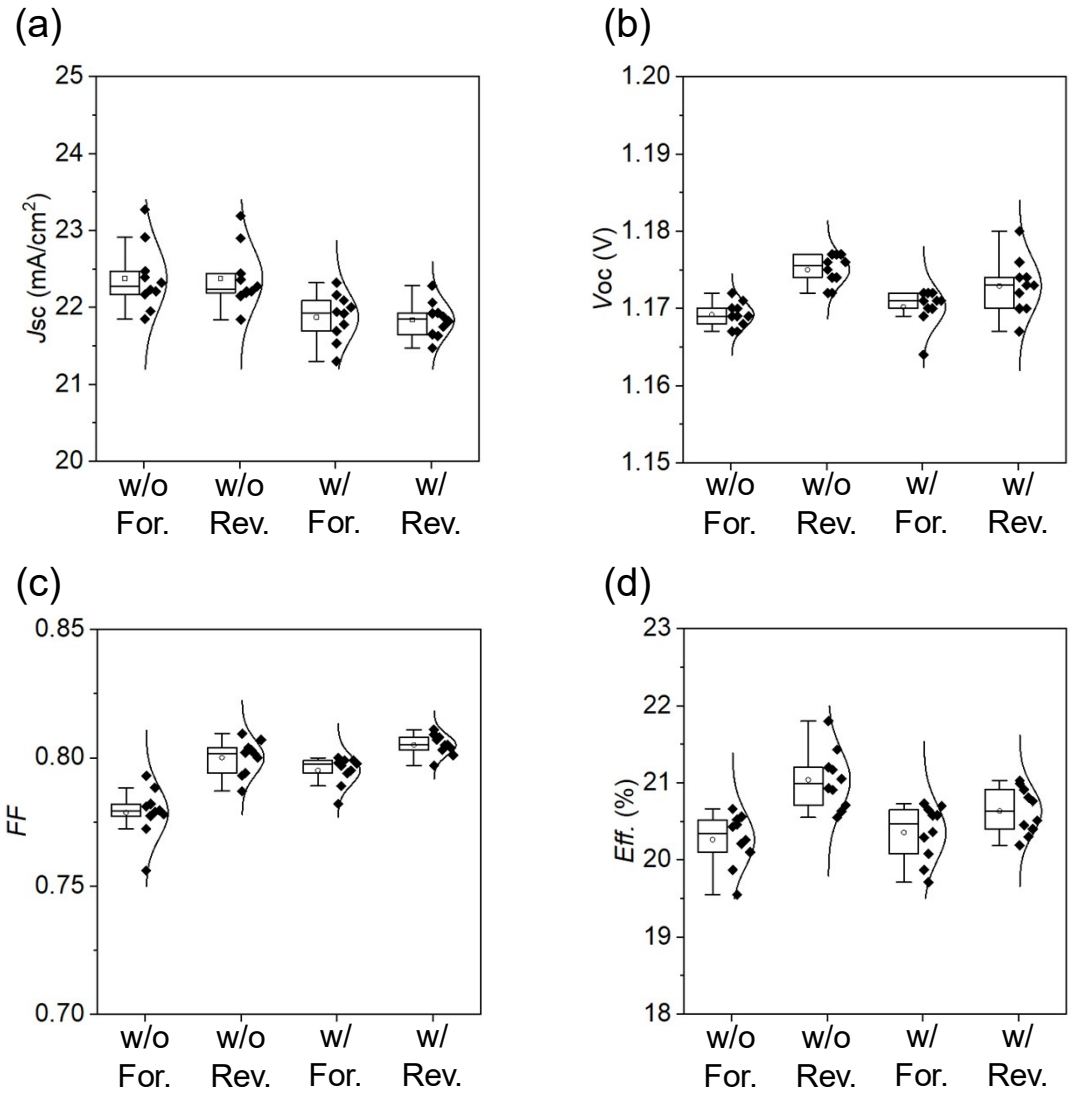

Fig. S9 Photovoltaic property distributions of perovskite solar cells with and without OHGaPc for (a) J_{sc}, (b) V_{oc}, (c) *FF*, and (d) PCE.

Table S1 Device performance of perovskite solar cells with different OHGaPc film thicknesses.

Thickness of OHGaPc film	Scan direction	Eff. (%)	J_{sc} (mA/cm^2)	V_{oc} (V)	*FF* (—)
without	For.	20.7	22.9	1.17	0.772
	Rev.	21.8	22.9	1.18	0.809
130 nm	For.	20.7	22.3	1.17	0.794
	Rev.	21.0	22.3	1.17	0.803
250 nm	For.	8.04	19.3	1.07	0.387
	Rev.	10.8	19.7	1.07	0.512
350 nm	For.	5.23	15.0	1.04	0.335
	Rev.	8.01	15.4	1.05	0.493
400 nm	For.	3.93	14.8	1.02	0.261
	Rev.	5.38	15.7	1.04	0.331
600 nm	For.	1.40	5.77	1.02	0.238
	Rev.	1.62	6.04	1.02	0.262

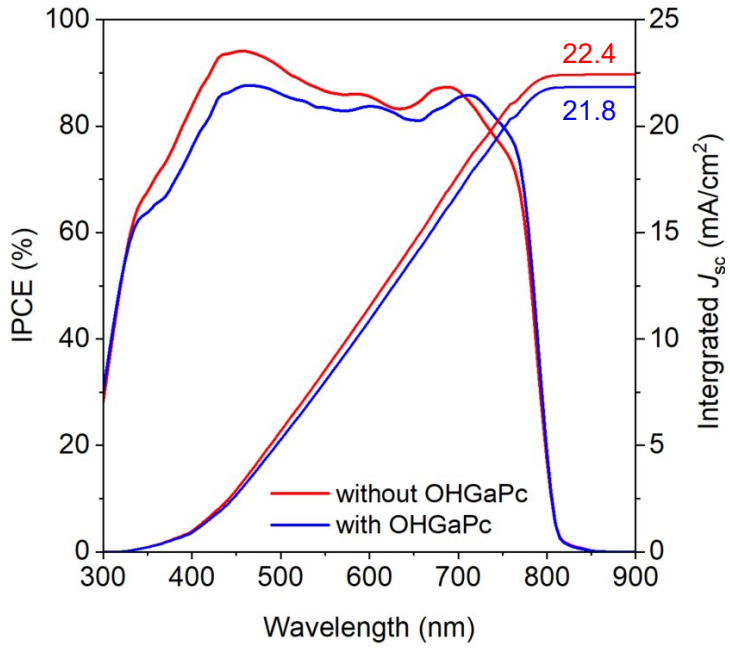

Fig. S10 IPCE spectra and integrated J_{sc} with and without OHGaPc.

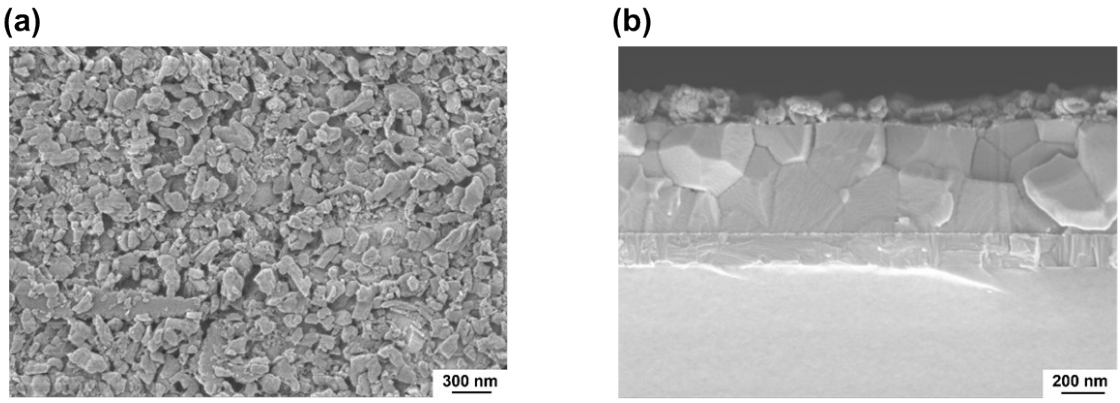

Fig. S11 SEM images of the (a) surface and (b) cross-section of the OHGaPC (thickness 130 nm).

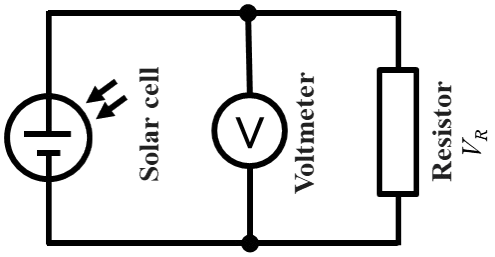

Fig. S12 Schematic of the circuit for the durability test device for perovskite solar cells.